Optimization of Series Inductance in Dual Active Bridge Converters Using Infinite-Width Bayesian Neural Networks

Hsiao-Chin Yen[1,*] Nguyen Tan Tung Man-Hay Pong Huang-Jen Chiu

[1]Department of Electronics and Computer Engineering, National Taiwan University of Science and Technology
* m11102282@mail.ntust.edu.tw

Abstract

This paper proposes a novel Bayesian optimization framework incorporating an Infinite-Width Bayesian Neural Network (BNN) for the optimal design of the series inductor in Dual-Active-Bridge (DAB) converters. First, a multi-constrained design space is formulated based on the topology and specifications of the DAB converter. Second, the objective function is defined to minimize the total power loss of the converter. Third, a Bayesian optimization procedure is developed using the Infinite-Width BNN as the surrogate model. This approach not only addresses the challenges of data scarcity and high computational cost in electromagnetic simulations but also improves the computational efficiency of the optimization process. Finally, the proposed Optimization framework is implemented through circuit-level and finite element analysis (FEA) tools, and the optimization result is validated via experimental results on a 5 kW hardware prototype.

Keywords: Design optimization, power converters, design automation.

I. INTRODUCTION

The Dual Active Bridge (DAB) DC-DC converter is used for many high-power applications, including electric vehicle (EV) charging, renewable energy integration, and energy storage systems. Its inherent features, including galvanic isolation, bidirectional power flow, and ZVS capability, make it a compelling choice for medium- to high-power conversion stages [1], [2]. Engineers need to improve converter efficiency based on knowledge and experience related to converter topology, magnetic components, and power electronics. With advancements in computational tools, engineers can now use circuit simulators or FEA software to obtain precise results, and numerous optimization algorithms have been surveyed [3].

Bayesian optimization has emerged as a powerful tool for design space exploration under limited evaluation budgets, particularly when dealing with black-box functions and expensive simulations, as is common in power electronics. By leveraging surrogate models to approximate objective functions such as converter loss, Bayesian optimization enables designers to find optimal solutions with significantly fewer simulations compared to grid or random search, previous studies have applied Bayesian optimization to the design of magnetic components [4], [5]. In the context of DAB converter design, many design variables need to be determined, such as the series inductor, transformer, and switching devices. However, conventional Gaussian Process (GP) models used in Bayesian optimization face scalability issues and often lack expressiveness in high-dimensional or physics-informed design spaces.

Motivated by the practical need for loss-aware and computationally efficient inductor design, and the theoretical strengths of infinite-width BNNs in surrogate modeling [6]-[8], this paper proposes an optimization framework for series inductance design in DAB converters. This work consists of three parts: first, the design space and constraints for series inductance are defined based on knowledge of DAB converter topology and the formulation of an optimization problem aimed at minimizing power loss; second, an infinite-width BNN is described and integrated into a Bayesian optimization loop to solve the optimization problem. The proposed method is implemented using a hybrid platform that combines circuit-level simulation and electromagnetic finite element analysis (FEA); third, the optimization process and simulation environment are described, followed by a demonstration of the optimization results. This work offers a pathway toward more intelligent and efficient design automation in power electronics.

II. OPTIMIZATION PROBLEM FORMULATION

2.1 DAB Converter and Control method

Before deciding on the design space and constraints for the series inductance, we first need to check the specifications and theoretical equations of the dual active bridge converter.

2.1.1 Specification and Topology

Table I shows the specifications of the dual active bridge we aim to optimize, and Fig. 1, provides the topology. Our optimization focuses on the series inductance L_s in Fig. 1,.

TABLE I: DUAL ACTIVE BRIDGE CONVERTER SPECIFICATION

Parameter	Value	Description
Power	5000 W	Rated output power
V_{in}	800 V	Input voltage
V_{out}	400 V	Output voltage

F_{sw}	100 - 200k Hz	Switching frequency
Control method	SPS	Single phase shift control

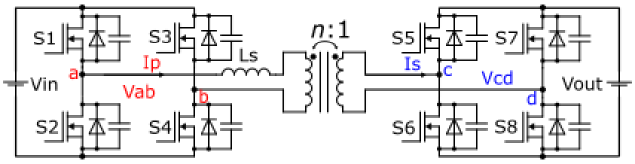

Fig. 1. A dual active bridge converter

Fig. 2, shows the key waveforms of the dual active bridge converter operating under single phase shift (SPS) control, where D represents the outer phase shift between the two active full bridges. By controlling the outer phase shift, the power flow from the primary side to the secondary side can be regulated.

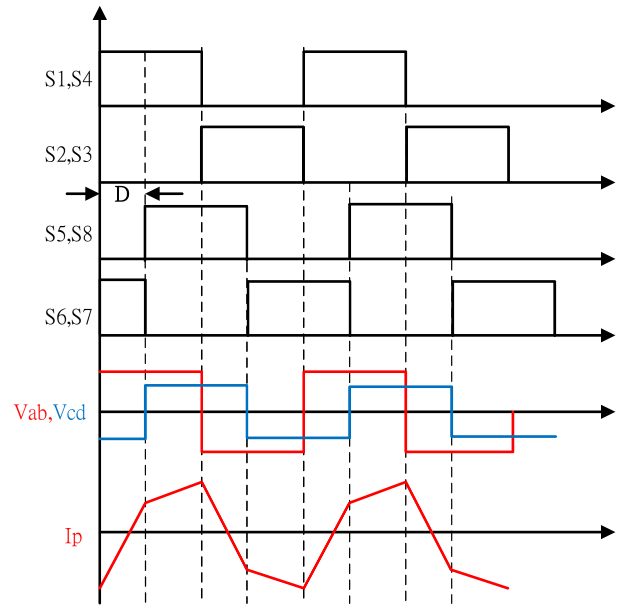

Fig. 2. The DAB converter key waveforms at SPS control

2.1.2 Converters' equations

This section provides the governing equations of the dual-active-bridge (DAB) converter. Because our objective is to optimize the series inductance L_s, we first establish the equations required for component selection and for defining the feasible design space and constraints of L_s.

Equation (1) establishes the relationship between the output power and the circuit parameters. This equation is based on the single phase shift (SPS) control of the DAB converter.

$$P = nV_{in}V_{out} \times \frac{(1-D)D}{2L_sF_{sw}} \qquad (1)$$

which P is Output power
n is transformer turn ratio
V_{in} is input voltage
V_{out} is output voltage
D is outer phase shift
L_s is series inductance
F_{sw} is switching frequency

Equation (2) gives the peak current on the primary side of the transformer, and Equation (3) gives the RMS current on the primary side, as derived in [9]. These two equations are used for switch selection, transformer winding selection, and series inductor winding selection.

$$I_{peak} = \frac{(2D-1)V_{in}+nV_{out}}{4F_{sw}L_s} \qquad (2)$$

$$I_{rms} = \frac{\sqrt{3}V_{in}}{12F_{sw}L_s} \times \sqrt{3A_1 - 2A_2 - 12A_3 - 4A_4 - 4A_5} \qquad (3)$$

$$where\ A_1 = D^2(d+1)^2, A_2 = D^3(d^2+1),$$

$$A_3 = dD_2(D-1), A_4 = dD_2^2(2D_2-3),$$

$$A_5 = d(3D-1), d = \frac{nV_{out}}{V_{in}}, D_2 = (1-D)$$

which n is transformer turn ratio
V_{in} is input voltage
V_{out} is output voltage
D is outer phase shift
L_s is series inductance
F_{sw} is switching frequency

At this high switching frequency, it is not core saturation but core loss that limits the number of primary turns. The transformer is designed based on Faraday's law, with the wire size selected according to the skin effect and the RMS current derived from Equation (3). Based on the design equations (1)–(3), we select the components and design the transformer to meet the specified requirements. Table II shows the fixed design parameters of the DAB converter.

TABLE II: DUAL ACTIVE BRIDGE CONVERTER FIX DESIGN PARAMETER

Component	Description
Input capacitor	C4AQPBW5100M3JJ
Output capacitor	C4AQCLW5200A36J
Switch	IMZC120R022M2HXKSA1
Transformer	PQ 50/50 / Hitachi ML26D / Primary wire: 25 turns 0.1mm x 250 Secondary wire: 13 turns 0.1mm x 250
Series inductor	PQ 40/40 / Hitachi ML24D / 0.08mm x 600

2.2 Design Space and Constraints for Series Inductance

There is a trade-off between the core loss of the magnetic components and the switching loss of the semiconductor devices when the switching frequency is varied. According to Equation (1), different switching frequencies correspond to different series inductance values, and varying the phase shift also results in different series inductances. Therefore, this section analyzes the design space of the series inductance for optimization to ensure that the entire design space meets the specified requirements.

The first parameter to be optimized is the switching frequency, for which the upper and lower bounds must be determined. The upper bound is limited by the switching loss of the semiconductor devices and by the core material data provided by the manufacturer. At high switching frequencies, total loss is dominated by switching loss; moreover, if the manufacturer does not provide a core-loss curve for the target frequency range, accurate results cannot be obtained from magnetic device simulations. The lower bound is determined by the core dimensions. According to Faraday's law, once the core cross-sectional area is fixed, the magnetic flux density must be kept sufficiently low to prevent excessive core loss. Equation (4) defines the design space for the switching frequency.

$$F_{sw} = [100,105,110,\dots,200]\ kHz \tag{4}$$

The core material and dimensions of the series inductor are taken from Table II, leaving two parameters to be determined: the number of turns and the air gap length. The upper bound of the number of turns is limited by the core window area and wire size, while the lower bound is constrained by core saturation and core loss. Using Equation (2) and Faraday's law, Fig. 3, is obtained. In Fig. 3,, N represents the minimum number of turns required to avoid core saturation, and the red line indicates the maximum number of turns allowed by the window area and wire size. The white dotted line in Fig. 4, shows that when N=18, all design parameters to the left of this line are valid, and the corresponding outer phase shift is D = 44.2°. Therefore, N is fixed at 18, and the phase shift range is set between 18.2°and 44.2°.

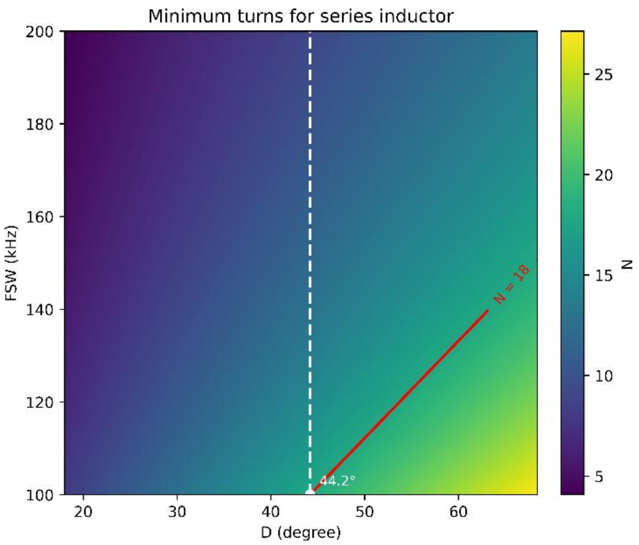

Fig. 3. Minimum turns for series inductor

To determine the range of series inductance for the DAB converter, Equation (1) is applied together with the circuit specifications in Table I. With the input voltage, output voltage, and rated power fixed, the corresponding series inductance required to achieve the rated power is calculated, considering a phase shift range between 18.2° and 44.2°. Fig. 4, shows the resulting series inductance range, where the upper bound is indicated by the red dot labeled max and the lower bound by the red dot labeled min. Note that the range of series inductance has already been adjusted to subtract the leakage inductance of the transformer.

The remaining parameter to be determined, and the second parameter to be optimized, is the air gap length. Since the number of turns is fixed, the desired series inductance value can be obtained by adjusting the air gap length. A parameter sweep is performed using the FEA tool to identify the range of air gap lengths that satisfy the upper and lower bounds of the series inductance shown in Fig. 4, Fig. 5, illustrates that the air gap length design space lies within the series inductance boundaries, and Equation (5) defines the feasible design space for the air gap length.

$$l_g = [0.5,0.6,0.7,\dots,5.5]\ mm \tag{5}$$

which l_g is airgap length

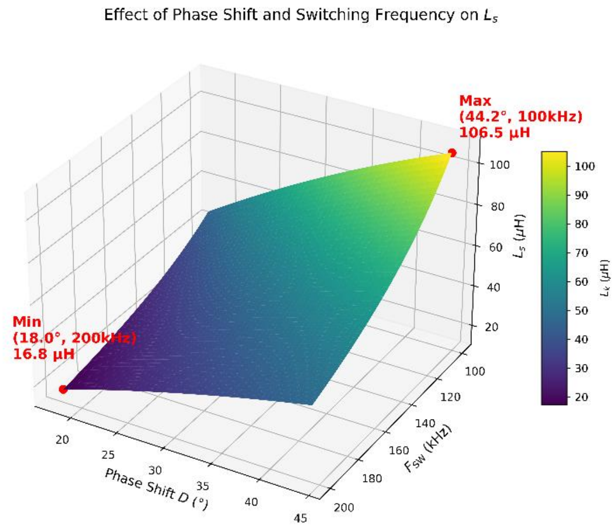

Fig. 4. Effect of Phase shift and Switching frequency on L_s

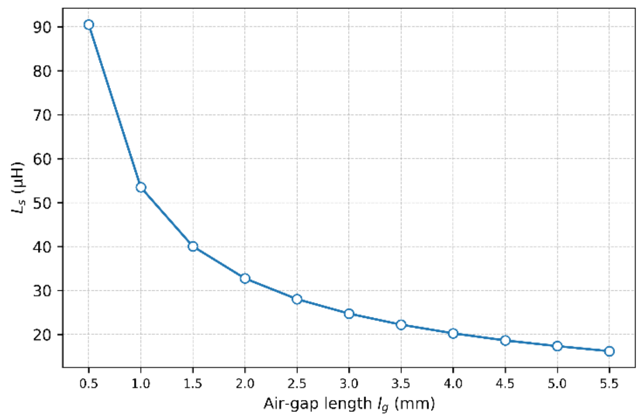

Fig. 5. Series Inductance value vs. Air gap length result from FEA tool

2.3 Objective Function Definition

Two parameters are optimized in this study: the air gap length and the switching frequency. The objective is to maximize the efficiency of the DAB converter. The black-box function represents the efficiency as a function of switching frequency and air gap length, and Equation (6) defines the objective function.

$$\max_{lg,F_{sw}} eff(l_g, F_{sw}) \quad (6)$$

$$subject\ to\ \ l_g \in [0.5,5.5]\ mm, F_{sw} \in [100k, 200k]\ Hz$$

which l_g is air gap length
eff is power converter efficiency
F_{sw} is switching frequency

III. BAYESIAN OPTIMIZATION FRAMEWORK

3.1 Overview of Bayesian Optimization

Bayesian Optimization (BO) is a sample-efficient global optimization technique particularly suited for optimizing expensive-to-evaluate, black-box functions with unknown analytical forms. Unlike gradient-based methods, BO does not require derivative information and instead builds a probabilistic surrogate model—typically a Gaussian Process (GP)—to approximate the objective function. This surrogate enables the algorithm to estimate both the expected performance and uncertainty of function evaluations across the domain.

At each iteration, an acquisition function, such as Expected Improvement (EI) or Upper Confidence Bound (UCB), guides the selection of the next evaluation point by balancing exploration (searching unexplored areas) and exploitation (refining near known optima). This strategy is especially advantageous in engineering, machine learning, and design optimization contexts where each function evaluation can be computationally intensive or costly, such as electromagnetic simulation or physical experimentation.

The objective function in Equation (7), which is normally treated as a black-box function, is used to demonstrate the Bayesian optimization process. Fig. 6, (a) shows the acquisition function after ten iterations, while Fig. 6, (b) presents the objective function, where the optimal region lies at the top-center-right of the figure. At this stage, the current observation points are concentrated in a suboptimal area, representing the exploitation phase of Bayesian optimization (refining near known optima). The algorithm then evaluates points far from this suboptimal region, representing the exploration phase (searching unexplored areas) to identify potentially better regions. After twenty iterations, as shown in Fig. 6, (c), Bayesian optimization locates the optimum region within the design space.

$$f(x1, x2) = \frac{(\sin(2.5x_1 - 2.5)\cos(2.5 - 5x_1) + \frac{(2.5x_1+0.5)^2}{10})}{5} + \frac{1}{5} \quad (7)$$

where $x_1 \in [-1, 1]$, $x_2 \in [-1,1]$

3.2 Surrogate Modeling with Infinite-Width BNNs

This paper employs infinite-width Bayesian neural networks (I-BNNs) and uses them as kernel functions for Bayesian optimization (BO). A fully connected neural network with L hidden layer, this neural network requires two sets of parameters: weight terms and bias terms. The weight terms are drawn from $N(0, \sigma_w)$, and bias terms are drawn from $N(0, \sigma_b)$. In the infinite-width limit, the output of this network is exactly equivalent to Gaussian Process [6]. This type of kernel is called I-BNN kernel. Different from other GP kernels for example matérn kernel, the I-BNN kernel is not based on Euclidean distance, allowing the GP to represent nonstationary functions.

The I-BNN kernel is employed for Bayesian optimization to locate the optimum point of Equation (7), with the I-BNN depth set to two layers, the weight variance to 0.1, and the bias variance to 0.05. Fig. 6, (d) shows the acquisition function after twenty iterations. The observation points are concentrated in the central area, which corresponds to a suboptimal region. Unlike the Matérn kernel results in Fig. 8,, the I-BNN kernel identifies additional bright regions in the upper part of the figure, indicating that it considers these areas to have potential for improvement.

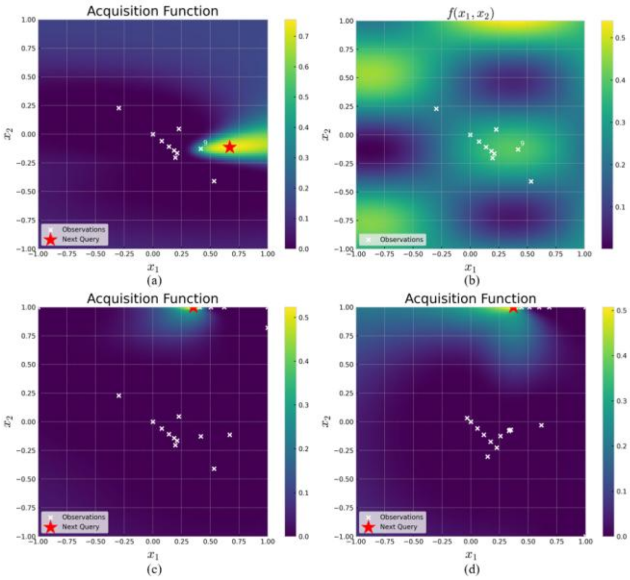

Fig. 6 (a) Acquisition function of BO using matérn kernel after ten iterations. (b) Objective function of equation (7). (c) acquisition function of BO using matérn kernel after twenty iterations. (d) acquisition function of BO using I-BNN kernel after twenty iterations.

IV. OPTIMIZATION PROCESS AND ENVIRONMENT SETUP

4.1 Optimization flow chart

Fig. 7, presents the optimization flowchart. The process begins with two initial points—one at the center of the design space and one selected randomly—which are simulated to construct the initial surrogate model for Bayesian optimization. The acquisition function then proposes new design parameters with a higher probability of improving efficiency. After 20–30 iterations, the optimal parameters are obtained. The stopping criteria are first meeting the efficiency specification or second reaching the computation time limit; in this work, the latter is used.

4.2 Simulation Environment

This section describes the detailed simulation environment. The simulations are performed using SIMBA, a tool designed for power electronics and motor drive applications. SIMBA offers good integration with Python, allowing it to be incorporated into our automated simulation workflow. Fig. 8, shows the dual active bridge circuit in the SIMBA simulator.

The FEA analysis is a main part in the simulation loop, using Ansys maxwell to simulate the inductance value of series inductor and leakage and magnetizing inductance of the transformer, and simulate the core loss and copper loss for both of the magnetic device, Fig. 9, show the 1/4 Symmetry model for series inductor and transformer, the 1/4 Symmetry model can accelerate the simulation and reduce overall simulation times.

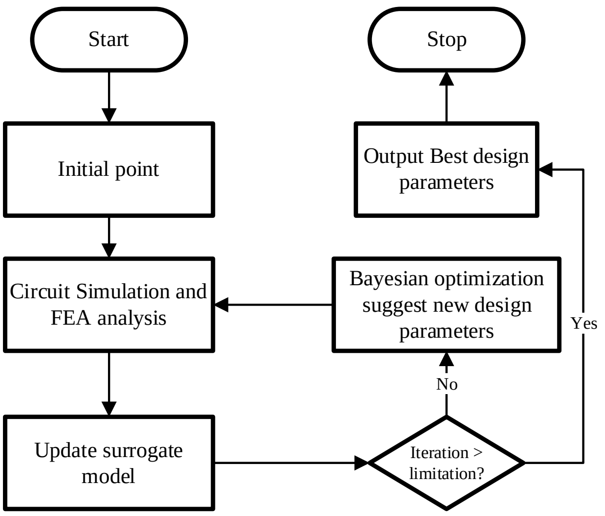

Fig. 7. Overview of optimization flow chart

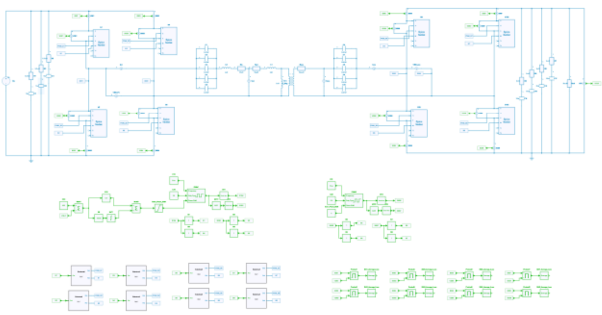

Fig. 8. Dual active bridge converter in SIMBA

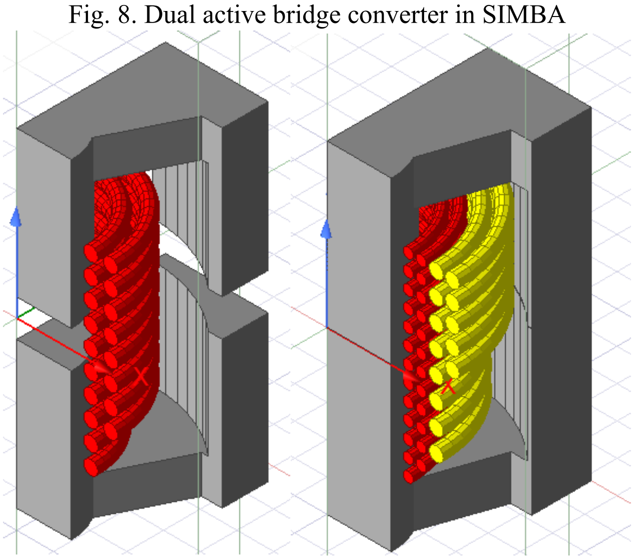

(a) (b)

Fig. 9. (a) 1/4 Symmetry model for series inductor
(b) 1/4 Symmetry model for transformer

The optimization algorithm, infinite-width Bayesian neural networks (I-BNNs), is implemented using BoTorch [10], a Bayesian optimization library built on PyTorch. BoTorch supports flexible and efficient optimization of expensive black-box functions using Gaussian processes and other surrogate models, making it well-suited for machine learning and engineering applications with costly evaluations. The overall optimization loop is automated in Python. Fig. 10, shows the detailed simulation environment.

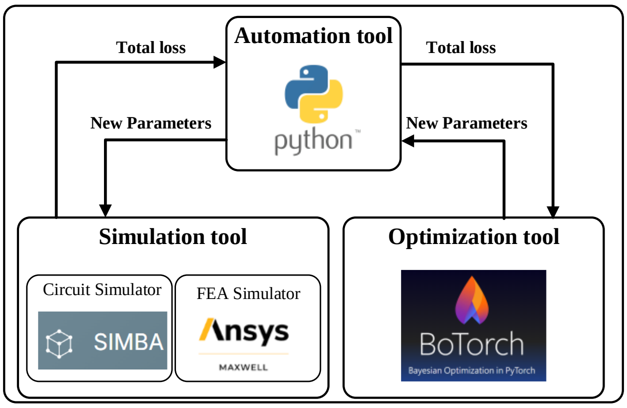

Fig. 10. Simulation environment

V. Results and Discussion

5.1 Optimization Result

By using the design space in equation (4) and equation (5) and running the optimization loop in Fig. 7,. The Bayesian optimization using infinite-width Bayesian neural network can find the optimal point in the design space. In Table III, the optimal design parameters is get at iteration 4^{th} (i = 4) which provide the highest efficiency. Therefore $\mathrm{lg} = 3.4\,mm$ and $f_{sw} = 100\,kHz$ is the best design parameters in this design.

TABLE III: Optimization Iteration Result

i	lg (mm)	f_{sw} (kHz)	Efficiency (%)
Init	3.5	150	97.500
1	1.5	200	96.744
2	3.6	150	97.348
3	3.3	150	97.358
4*	**3.4**	**100**	**97.735**
5	3.5	100	97.733
6	3.3	100	97.720
7	3.6	100	97.725
8	3.8	100	97.727
9	3.7	100	97.728
10	4.3	100	97.734
11	4.5	100	97.729

5.2 Experiment Result

The best design parameters listed in Table III are implemented in a DAB converter prototype. Fig. 11, shows the hardware prototype, while Fig. 12, presents the operating waveforms. The prototype achieves a peak efficiency of 98.38%.

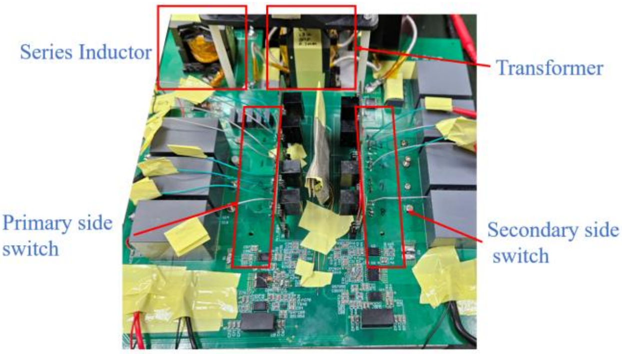

Fig. 11. 5kW Dual active bridge prototype

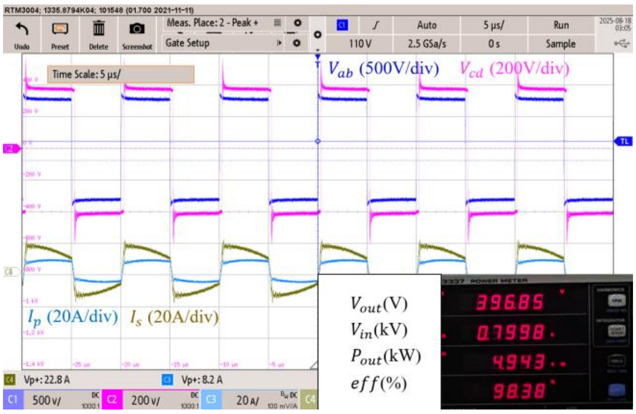

Fig. 12. Waveform and efficiency result of DAB prototype

VI. Conclusion

This paper proposes a new optimization structure for Bayesian optimization by using an infinite-width Bayesian neural network as a surrogate model, which gives BO a more flexible and new method for solving optimization problems in power converter design. This paper demonstrates how to decide the design space for the dual active bridge converter, explains the difference between the traditional surrogate model and the I-BNN surrogate model, and explains the optimization loop for the power converter. Finally, the best design parameters obtained from the optimization are implemented on a hardware prototype, and the peak efficiency is measured at 98.38%.

Acknowledgment

Thanks to the National Science and Technology Council (NSTC) in Taiwan Proj NSTC 113-2221-E-011 -108-MY2 for funding support. Thanks to the Advanced Power Electronics Lab in NTUST for providing excellent test facilities and software for this project. Also thanks to SIMBA for providing excellent power electronic simulation software and technical support.

References

[1] L. Li, G. Xu, D. Sha, Y. Liu, Y. Sun and M. Su, "Review of Dual-Active-Bridge Converters With Topological Modifications," in IEEE Transactions on Power Electronics, vol. 38, no. 7, pp. 9046-9076, July 2023.

[2] O. Zayed, A. Elezab, A. Abuelnaga and M. Narimani, "A Dual-Active Bridge Converter With a Wide Output Voltage Range (200–1000 V) for Ultrafast DC-Connected EV Charging Stations," in IEEE Transactions on Transportation Electrification, vol. 9, no. 3, pp. 3731-3741, Sept. 2023.

[3] M. Delhommais, "Review of optimization methods for the design of power electronics systems," 2020 22nd European Conference on Power Electronics and Applications (EPE'20 ECCE Europe), Lyon, France, 2020, pp. 1-10.

[4] N. T. Tung, M. -H. Pong and H. -J. Chiu, "Magnetics Design Optimization for LLC Converter employing Machine Learning," 2023 11th International Conference on Power Electronics and ECCE Asia (ICPE 2023 - ECCE Asia), Jeju Island, Korea, Republic of, 2023, pp. 1219-1224.

[5] T. -H. Huang, K. -E. Lu, N. T. Tung, M. H. Pong and H. -J. Chiu, "Flyback Converter Transformer Design Optimization by AI," 2024 Tenth International Conference on Communications and Electronics (ICCE), Danang, Vietnam, 2024, pp. 303-308.

[6] Y. Cho, and L. Saul. Kernel Methods for Deep Learning. Advances in Neural Information Processing Systems 22, 2009.

[7] J. Lee, Y. Bahri, R. Novak, S. Schoenholz, J. Pennington, and J. Dickstein. Deep Neural Networks as Gaussian Processes. International Conference on Learning Representations 2018.

[8] Y.L. Li, T.G.J. Rudner, A.G. Wilson. A Study of Bayesian Neural Network Surrogates for Bayesian Optimization. International Conference on Learning Representations 2024.

[9] M. Kim, M. Rosekeit, S. -K. Sul and R. W. A. A. De Doncker, "A dual-phase-shift control strategy for dual-active-bridge DC-DC converter in wide voltage range," 8th International Conference on Power Electronics - ECCE Asia, Jeju, Korea (South), 2011, pp. 364-371.

[10] M. Balandat, B. Karrer, D. R. Jiang, S. Daulton, B. Letham, A. Wilson, and E. Bakshy, "BoTorch: A framework for efficient Monte-Carlo Bayesian optimization," in Advances in Neural Information Processing Systems, vol. 33, pp. 21524–21538, 2020.